

# Theory of Bernstein Modes in Graphene

R. Roldán<sup>1,2</sup>, M. O. Goerbig<sup>2</sup>, and J.-N. Fuchs<sup>2</sup>

<sup>1</sup>*Institute for Molecules and Materials, Radboud University Nijmegen, Heyendaalseweg 135, 6525 AJ Nijmegen, The Netherlands*

<sup>2</sup>*Laboratoire de Physique des Solides, Univ. Paris-Sud, CNRS, UMR 8502, F-91405 Orsay Cedex, France*

(Dated: February 24, 2024)

We present a theoretical description of Bernstein modes that arise as a result of the coupling between plasmon-like collective excitations (upper-hybrid mode) and inter-Landau-level excitations, in graphene in a perpendicular magnetic field. These modes, which are apparent as avoided level crossings in the spectral function obtained in the random-phase approximation, are described to great accuracy in a phenomenological model. Bernstein modes, which may be measured in inelastic light-scattering experiments or in photo-conductivity spectroscopy, are a manifestation of the Coulomb interaction between the electrons and may be used for a high-precision measurement of the upper-hybrid mode at small non-zero wave vectors.

PACS numbers: 78.30.Na, 73.43.Lp, 81.05.ue

## I. INTRODUCTION

Most of the electronic properties of graphene, two-dimensional (2D) graphite, may be understood within the picture of non-interacting or weakly-correlated massless Dirac particles.<sup>1</sup> A notable exception is the recently observed fractional quantum Hall effect,<sup>2,3</sup> which arises in a strong magnetic field when a Landau level (LL) is only partially filled and when the Coulomb interaction becomes the relevant energy scale due to a quenched kinetic energy, similarly to the usual 2D electron gas in semiconductor heterostructures. Apart from this rather particular situation, the role of the Coulomb interactions may be quantified with the help of the graphene fine-structure constant  $\alpha_G \equiv e^2/\hbar v_F \simeq 2.2/\epsilon$ , in terms of the Fermi velocity  $v_F \simeq 10^6$  m/s and the dielectric constant  $\epsilon$  of the surrounding medium.

Even if the value of  $\alpha_G$  indicates that graphene should be a moderately correlated material, experimental indications for the role of Coulomb interactions in the absence of a magnetic field are rather sparse. Recent angular-resolved photoemission experiments have revealed features that hint at “plasmaron” excitations that may be viewed as quasi-particles dressed by interaction-induced plasmon excitations.<sup>4</sup> Furthermore, an indirect determination of the screened fine structure constant, defined as  $\alpha_G^*(\mathbf{q}, \omega) = e^2/\hbar v_F \epsilon(\mathbf{q}, \omega)$ , where the dynamic screening due to inter-band processes is encoded into the dielectric function  $\epsilon(\mathbf{q}, \omega)$ , has been measured by means of X-ray scattering in graphite.<sup>5</sup> In the  $\omega \rightarrow 0$  and long wavelength limit, the value given in Ref. 5 for graphene (extracting indirectly the polarization of graphene from measurements on graphite) is  $\alpha_G^* \simeq 0.14$ , i.e. a value that is roughly one order of magnitude smaller than the one mentioned above, for the case of freestanding graphene ( $\epsilon = 1$ ). The investigation of interaction-related effects may therefore be viewed as one of the major issues in fundamental research on graphene.

Interaction effects are expected to play a role in graphene exposed to a strong perpendicular magnetic

field in the form of plasmon-like excitations.<sup>6–10</sup> Most saliently, the relativistic character of the electrons in graphene gives rise to rather exotic linear magneto-plasmons,<sup>9</sup> in addition to the upper-hybrid mode (UHM) which is a mixture of the cyclotron mode and the usual 2D plasmon with its low-energy  $\sqrt{q}$  dispersion, in terms of the wave vector  $q$ . In the context of the 2D electron gas in semiconductor heterostructures, the UHM is coupled via the Coulomb interaction to inter-LL excitations, and their hybridization gives rise to avoided level crossings, known as Bernstein modes.<sup>11</sup> Bernstein modes have been measured in photo-conductivity spectroscopy and inelastic light-scattering experiments,<sup>12–16</sup> and these techniques may in principle also be applied to graphene.

In this paper, we study theoretically the Bernstein modes in graphene. These Bernstein modes become apparent in the spectral function, which takes into account the Coulomb interaction between the electrons in the random-phase approximation (RPA). We propose a phenomenological model that captures the relevant features, as the position and size of the anticrossings between the UHM and the inter-LL excitations, that appear in the excitation spectrum of this system. Moreover, our results could be used to analyze future experimental results and to identify the different modes. For this aim, we propose two different experimental setups that could be applied to graphene in order to measure the Bernstein modes as well as the dispersion relation of the UHM in this material. In contrast to 2D electrons in semiconductor heterostructures with a parabolic band dispersion and an equidistant LL spacing, one observes a plethora of inter-LL transitions in graphene as a consequence of the  $\lambda\sqrt{Bn}$  scaling of the relativistic LLs, where  $\lambda = +$  or  $-$  for the conduction and the valence band, respectively, and the integer  $n$  denotes the LL index. This results in a large number of intersections between the inter-LL transitions and the UHM, such that a measurement of the Bernstein modes would in principle allow for a high-precision determination of the dispersion relation of the upper-hybrid mode.

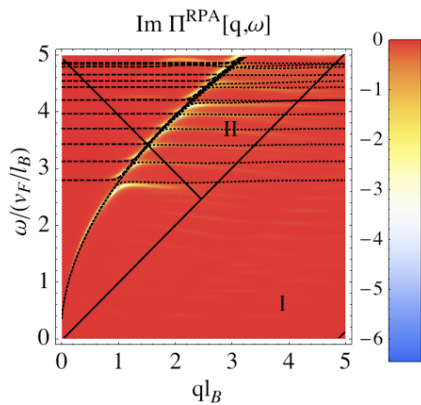


FIG. 1. (Color online) RPA Spectral function for electrons in graphene, with  $N_F = 3$ ,  $\delta = 0.02v_F/l_B$ , for a fine-structure constant  $\alpha_G = 1$ . The dashed black lines are obtained from the expression (8) for the coupled modes, for the same parameters and  $\gamma = 3/4$ . The continuous lines delimit the region for intra-band (I) and that for inter-band (II) excitations.

The paper is organized as follows. In Sec. II, we discuss the Bernstein modes which are visible in the RPA spectral function (Sec. II A) and propose a phenomenological model (Sec. II B) that allows for a quantitative description of the position and the strength of the modes. Section III is devoted to possible experimental observations of Bernstein modes in graphene, and we present our conclusions in Sec. IV.

## II. THEORETICAL DESCRIPTION OF BERNSTEIN MODES IN GRAPHENE

### A. Bernstein modes in the RPA spectral function

Quite generally, the collective charge excitations generated by the Coulomb interaction between the electrons may be obtained from the zeros of the RPA dielectric function

$$\epsilon_{RPA}(\omega, \mathbf{q}) = 1 - \frac{2\pi e^2}{\epsilon|\mathbf{q}|} \Pi^0(\omega, \mathbf{q}), \quad (1)$$

in terms of the polarizability  $\Pi^0(\omega, \mathbf{q})$  for non-interacting 2D electrons. For electrons in graphene in the integer quantum Hall regime, the polarizability reads (we use a system of units with  $\hbar \equiv 1$ )<sup>7,9</sup>

$$\begin{aligned} \Pi^0(\omega, \mathbf{q}) = & \sum_{\lambda n, \lambda' n'} \frac{g[n_F(\lambda n) - n_F(\lambda' n')]}{\omega'(\lambda\sqrt{n} - \lambda'\sqrt{n'}) + \omega + i\delta} \\ & \times \frac{|\mathcal{F}_{\lambda n, \lambda' n'}(\mathbf{q})|^2}{2\pi l_B^2}, \end{aligned} \quad (2)$$

where  $n_F(\lambda n)$  is the Fermi distribution function,  $\omega' \equiv \sqrt{2}v_F/l_B$  is the characteristic LL frequency,  $g = 4$  represents the four-fold spin-valley degeneracy, and  $\delta$  takes into account the disorder-induced LL broadening on a

phenomenological level. The form factors  $\mathcal{F}_{\lambda n, \lambda' n'}(\mathbf{q})$  are due to the graphene-LL wave functions and take into account the chirality of the carriers. They may be expressed in terms of the cyclotron variable  $\boldsymbol{\eta} = \mathbf{r} - \mathbf{R}$ , where  $\mathbf{r}$  is the position of the electron and  $\mathbf{R}$  that of the center of the cyclotron motion, which is a constant of motion,

$$\begin{aligned} \mathcal{F}_{\lambda n, \lambda' n'}(\mathbf{q}) = & 1_n^* 1_{n'}^* \langle n-1 | e^{-i\mathbf{q}\cdot\boldsymbol{\eta}} | n'-1 \rangle \\ & + \lambda\lambda' 2_n^* 2_{n'}^* \langle n | e^{-i\mathbf{q}\cdot\boldsymbol{\eta}} | n' \rangle, \end{aligned} \quad (3)$$

and we have used the short-hand notation  $1_n^* \equiv \sqrt{(1 - \delta_{n,0})/2}$  and  $2_n^* \equiv \sqrt{(1 + \delta_{n,0})/2}$ . The states  $|n\rangle$  are the usual eigenstates of the harmonic-oscillator operators,  $a^\dagger a|n\rangle = n|n\rangle$ , where  $a = (\eta_x + i\eta_y)/\sqrt{2}l_B$ .

The spectral function, i.e. the imaginary part of the RPA polarizability  $\Pi^0(\omega, \mathbf{q})/\epsilon_{RPA}(\omega, \mathbf{q})$ , is shown in Fig. 1, where we have chosen, for illustration reasons, a value of  $\alpha_G = 1$  for the graphene fine-structure constant. The Fermi level  $E_F = \lambda\omega'\sqrt{N_F}$  is fixed in the LL  $N_F = 3$  in the conduction band ( $\lambda = +$ ), and we have chosen an impurity broadening of  $\delta = 0.02v_F/l_B$ . The main spectral weight is concentrated in the UHM, which disperses as<sup>17</sup>

$$\omega_{uh}(q, B) = \sqrt{\omega_p^2(q) + \omega_C^2(B)} \quad (4)$$

and which may be viewed as the high-field descendent of the  $B = 0$  2D plasmon with the approximate dispersion relation<sup>18-20</sup>

$$\omega_p(q) \simeq \sqrt{\frac{2e^2 E_F}{\epsilon} q + \gamma v_F^2 q^2}. \quad (5)$$

The first term in this expression yields the usual  $\sqrt{q}$  dispersion of the classical plasmon,<sup>21</sup> which is clearly visible in Fig. 1, while the second one represents a higher-order correction due to quantum effects. The small- $q$  expansion of the RPA polarization function yields a negative prefactor for the quantum corrections,  $\gamma = -\alpha_G^2$ <sup>20</sup>, in contrast to non-relativistic electrons. It seems, however, that  $\gamma$  depends itself on  $q$  and  $\alpha_G$ , namely at larger values of the wave vector where  $\gamma$  crosses over to positive values. Here, we use  $\gamma$  as a fitting parameter to our RPA results in Fig. 1, where the UHM is best described by the value  $\gamma = 3/4$  as noted by Shung,<sup>18</sup> in the shown wave-vector range and for an interaction parameter of  $\alpha_G = 1$ . The main effect of the magnetic field is the  $q = 0$  gap, which the plasmon acquires and that is given by the density-dependent cyclotron gap  $\omega_C(B) = eBv_F^2/E_F$  in Eq. (4).

It is clearly visible in Fig. 1 that, although the main part of the spectral weight is found in the upper-hybrid mode, this mode is not a continuous line. Instead, one notices a series of avoided level crossings whenever the upper-hybrid mode coincides with the energy of a dispersionless inter-LL transition,  $\Omega_{\lambda n, n'} = \omega'(\sqrt{n'} - \lambda\sqrt{n})$ , where an electron is promoted from the LL  $n$  in the band  $\lambda$  to  $n'$  in the conduction band (above the Fermi level). These avoided level crossings are nothing other than the

Bernstein modes, which occur at the wave vectors

$$ql_B = \frac{1}{\gamma} \sqrt{2N_F} \quad (6)$$

$$\times \left\{ \sqrt{\alpha_G^2 + \gamma \left[ \frac{(\sqrt{n'} - \lambda\sqrt{n})^2}{N_F} - \frac{1}{4N_F^2} \right]} - \alpha_G \right\}$$

in graphene.

## B. Phenomenological model

In order to describe the coupling between the UHM and the inter-LL excitations within a phenomenological model, we treat the UHM as a bosonic excitation, described by the Hamiltonian

$$H_{uh} = \sum_{\mathbf{q}} \omega_{uh}(q, B) b_{\mathbf{q}}^{\dagger} b_{\mathbf{q}}.$$

Here, the boson operator  $b_{\mathbf{q}}^{(\dagger)}$  is proportional to the Fourier component  $\rho_{uh}(\mathbf{q})$  of the density operator that constitutes the plasmon-type mode. This mode is coupled via the Coulomb interaction

$$H_{coupl} = \frac{1}{4} \sum_{\mathbf{q}} \frac{2\pi e^2}{\epsilon|\mathbf{q}|} [\rho(-\mathbf{q})\rho_{uh}(\mathbf{q}) + \rho_{uh}(-\mathbf{q})\rho(\mathbf{q})],$$

to the inter-LL excitations described by the density components

$$\rho(\mathbf{q}) = \sum_{\lambda n, \lambda' n'} \mathcal{F}_{\lambda n, \lambda' n'}(\mathbf{q}) \sum_{m, m'} \langle m | e^{-i\mathbf{q}\cdot\mathbf{R}} | m' \rangle c_{\lambda n, m}^{\dagger} c_{\lambda' n', m'},$$

in terms of the fermionic electron operators  $c_{\lambda n, m}^{(\dagger)}$ . This means that the electronic density is separated into a part that forms the UHM and another one that describes the inter-LL excitations, and formally one needs to introduce a constraint to avoid double counting of the electronic degrees of freedom.

The Coulomb coupling between the UHM and the LL excitations yields a renormalization of  $\omega_{uh}$  that may be calculated via a Dyson equation for the dressed propagator of the UHM, similarly to the magneto-phonon resonance discussed in Ref. 22. The avoided level crossing is then governed by the polarizability (2), which is dominated by the resonant term with  $\omega \simeq \omega_{uh} \simeq \Omega_{\lambda n, n'}$ , and the equation giving the poles of the dressed propagator reduces to

$$[\omega^2 - \omega_{uh}^2][\omega^2 - \Omega_{\lambda n, n'}^2] = \frac{g\mathcal{V}^2}{4} \omega_{uh} \Omega_{\lambda n, n'}, \quad (7)$$

where  $\mathcal{V} \equiv (e^2/\epsilon q l_B^2) |\mathcal{F}_{\lambda n, n'}(\mathbf{q})|^2$  is the effective coupling constant. From Eq. (7), one obtains the two solutions

$$\omega_{\pm}^2 = \frac{\omega_{uh}(q)^2 + \Omega_{\lambda n, n'}^2}{2} \quad (8)$$

$$\pm \sqrt{\frac{[\omega_{uh}^2 - \Omega_{\lambda n, n'}^2]^2}{4} + \frac{g\mathcal{V}^2}{4} \omega_{uh} \Omega_{\lambda n, n'}}.$$

The solutions are plotted in Fig. 1 in the form of dashed black lines, and one notices the good agreement with the maxima of spectral weight obtained from Eq. (2). At resonance  $[\omega_{uh}(q) \simeq \Omega_{\lambda n, n'}]$ , Eq. (8) may be linearized,

$$\frac{\omega_{\pm}}{v_F/l_B} \simeq (\sqrt{2n'} - \lambda\sqrt{2n}) \pm \frac{\delta_{\lambda n, n'}(q)}{2},$$

in terms of the relative splitting parameter

$$\delta_{\lambda n, n'}(q) = \frac{\sqrt{g}\mathcal{V}}{v_F/l_B} = \sqrt{g} \frac{\alpha_G}{q l_B} |\mathcal{F}_{\lambda n, n'}(\mathbf{q})|^2. \quad (9)$$

One notices in Fig. 1 that the UHM couples more strongly to inter-LL excitations that emerge from the inter-band regime (region II), with  $\lambda = -$ , than to those associated with intra-band transitions (region I). Indeed, the relative splitting parameter (9) is proportional to the  $|\mathcal{F}_{\lambda n, n'}(\mathbf{q})|^2$ , which is important in the regions of the spectrum which correspond to the particle-hole continuum in the absence of the magnetic field.<sup>9,10</sup> Because the UHM does not enter the intra-band region (I) of this continuum, the coupling to the corresponding inter-LL excitations (with  $\lambda = +$ ) is strongly suppressed, in contrast to those in the inter-band part of the particle-hole continuum, where the upper-hybrid mode enters.

## III. DISCUSSION AND IMPLICATIONS FOR EXPERIMENTS

Experimentally, Bernstein modes have been observed in 2D electron systems in semiconductor heterostructures.<sup>12-16</sup> In contrast to three-dimensional metals,<sup>23</sup> the main difficulty stems from the vanishing plasmon dispersion at  $q = 0$ , such that a direct measurement of Bernstein modes in homogeneous 2D systems via spectroscopic means is impossible. It is therefore necessary to impose a non-zero value of the wave vector to the system. Two different techniques have been successfully used to do so. The first one consists of a grated coupler, with a well-defined periodicity  $a$ , parallel and in close vicinity to the 2D electron gas.<sup>12-15</sup> The wave vector  $q_0 = 2\pi/a$  in the 2D electron gas, at which one may measure the electromagnetic response, is thus fixed by the periodicity of the grid via an electromagnetic coupling effect. This allows one to measure collective charge excitations via transmission spectroscopy (in the far-infrared regime) at a characteristic (non-zero) value of  $q$ .

An alternative technique consists of inelastic light-scattering experiments at a well-defined angle  $\theta$  between the incident photon and the vector perpendicular to the 2D electron gas.<sup>16</sup> In a light-scattering process, the photon thus transfers a momentum  $q_0 = \Delta\omega \sin\theta/c$  to the electrons, where  $\Delta\omega = (\omega_i - \omega_s)$  is the energy difference between the incident and the scattered photon, and  $c$  is the velocity of light. A resonance at the wave vector  $q$  and energy  $\Delta\omega$  is then interpreted as a collective charge excitation, such as a plasmon.

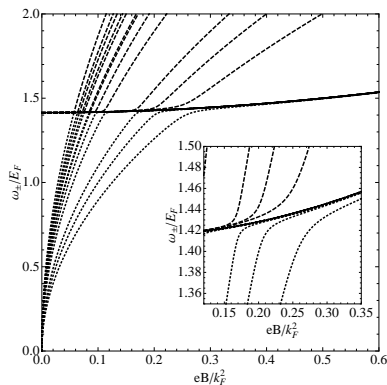


FIG. 2. Bernstein modes as a function of the magnetic field obtained from Eq. (8), for a fixed value of  $q_0/k_F = 1$  and  $\alpha_G = 1$ . Dashed lines represent inter-LL excitations, and the continuous line shows the UHM. The inset shows a zoom on the high-field region of the avoided level crossings.

In both techniques, which may in principle also be applied to graphene, it turns out to be simpler to study the Bernstein modes at the resonance condition (6) as a function of the magnetic field while keeping the wave vector fixed. One notices two essential differences of graphene with respect to a non-relativistic 2D electron gas in semiconductor heterostructures. First, because the electrons in graphene reside at the surface, the system has the advantage of being directly accessible by surface spectroscopic means, as e.g. scanning tunneling microscopy. Second, as a consequence of the non-equidistant LL spacing in graphene, the inter-LL transitions are not multiples of the fundamental cyclotron frequency  $\omega_C = eB/m_B$ , in terms of the band mass  $m_B$  of the semiconducting host material. Indeed, in a 2DEG there are, in general, many electron-hole transitions contributing to the same energy, due to the equidistant LLs. However, each particle-hole process contributes to a different energy in graphene because of the  $\sqrt{Bn}$  dispersion of graphene LLs. As a consequence, within the same energy window, there is a higher number of anticrossings between the UHM and the inter-LL transitions (Bernstein modes) in graphene as compared to a 2DEG.<sup>10</sup> Because the UHM is determined by the avoided level crossings with inter-LL excitations, this would, in principle, allow for a more precise measurement of the UHM in graphene as compared to non-relativistic electron systems.

In Fig. 2, we have plotted the solutions (8) of the Bernstein modes as a function of the magnetic field instead of the wave vector in order to make a closer connection with possible experiments. The wave vector is fixed at  $q_0/k_F = 1$  and we have chosen again  $\alpha_G = 1$  for illustration reasons. Notice that, in contrast to the above discussion, the natural units are no longer  $v_F/l_B$  for the energy and  $l_B^{-1}$  for the wave vector but the density-dependent Fermi energy  $E_F = v_F k_F$  and Fermi wave vector  $k_F = \sqrt{4\pi n_{el}}/g = \sqrt{\pi n_{el}}$ . Both units are therefore fixed by the carrier density  $n_{el}$ , whereas the in-

dex  $N_F$  changes as a function of the magnetic field as  $N_F \simeq k_F^2 l_B^2 / 2$ , where we have neglected the discreteness of  $N_F$ . The inter-LL excitations now disperse as  $\sqrt{B}(\sqrt{n} + \sqrt{n'})$ , whereas the UHM is only weakly dispersing in the plotted magnetic-field range. As one expects from Eq. (9), the Bernstein modes are most prominent at high magnetic fields, and the position of the avoided level crossings are easily obtained from Eq. (6). Neglecting the quantum corrections to the plasmon frequency ( $\gamma \rightarrow 0$ ) in the small wave-vector limit ( $q_0/k_F \lesssim 2\alpha_G/\gamma$ ), the Bernstein modes are expected at the field values

$$(eB)^{-1} \simeq \frac{(\sqrt{n'} - \lambda\sqrt{n})^2}{2\alpha_G q_0 k_F} + \sqrt{\frac{(\sqrt{n'} - \lambda\sqrt{n})^4}{4\alpha_G^2 q_0^2 k_F^2} + \frac{1}{2\sqrt{2}\alpha_G q_0 k_F^3}}. \quad (10)$$

Notice that the zero-field limit of the dispersion of the UHM, which one may extrapolate from the measurement of the Bernstein modes, gives direct access to the bare graphene fine-structure constant  $\alpha_G$ . Indeed, if one expresses Eq. (5) in terms of  $k_F$  and  $\alpha_G$ ,  $[\omega_{uh}(q, B \rightarrow 0)/v_F]^2 = 2\alpha_G k_F q$ , one may determine the fine-structure constant in the small- $q$  limit from the expression

$$\alpha_G = \frac{1}{2\sqrt{\pi n_{el}} q_0} \frac{\omega_{uh}^2(q_0, B \rightarrow 0)}{v_F^2}, \quad (11)$$

However, we emphasize that it is the unscreened graphene fine-structure constant which occurs in these expressions and not the screened one  $\alpha_G^*$ . Naturally, the information about  $\alpha_G$  is also encoded in the size of the mode splitting (9), but it seems more delicate to extract because of the complicated  $B$ -field and  $q$  dependence of the form factor.

#### IV. CONCLUSIONS

In conclusion, we have theoretically analyzed the Bernstein modes in graphene, which arise as a consequence of the interaction between plasmon-type modes and inter-LL excitations. The proposed model captures the position and strength of the couplings, as compared to the numerical solution of the RPA polarizability. Finally, we have shown that a possible measurement of Bernstein modes with the help of techniques that have been successfully used in conventional 2D electron systems with a parabolic band dispersion<sup>12–16</sup> and that may equally be used in graphene would allow for a measurement of the dispersion relation of the UHM.

#### ACKNOWLEDGMENTS

We acknowledge H. Bouchiat and M. I. Katsnelson for fruitful discussions. This work was funded by “Tri-

angle de la Physique”, the EU-India FP-7 collabora-

tion under MONAMI, and the ANR project NANOSIM GRAPHENE under Grant No. ANR-09-NANO-016.

- 
- <sup>1</sup> For a recent review on graphene, see. A. H. C. Neto, F. Guinea, N. M. R. Peres, K. Novoselov, and A. K. Geim, *Rev. Mod. Phys.* **81**, 109 (2009).
- <sup>2</sup> X. Du, I. Skachko, F. Duerr, A. Luican, and E. Y. Andrei, *Nature(London)* **462**, 192 (2009).
- <sup>3</sup> K. I. Bolotin, F. Ghahari, M. D. Shulman, H. L. Stormer, and P. Kim, *Nature* **462**, 196 (2009).
- <sup>4</sup> A. Bostwick, F. Speck, T. Seyller, K. Horn, M. Polini, A. H. MacDonald, and E. Rothenberg, *Science* **328**, 999 (2010).
- <sup>5</sup> J. P. Reed, B. Uchoa, Y. I. Joe, Y. Gan, D. Casa, E. Fradkin, and P. Abbamonte, *Science* **330**, 805 (2010).
- <sup>6</sup> A. Iyengar, J. Wang, H. A. Fertig, and L. Brey, *Phys. Rev. B* **75**, 125430 (2007).
- <sup>7</sup> K. Shizuya, *Phys. Rev. B* **75**, 245417 (2007).
- <sup>8</sup> Y. A. Bychkov and G. Martinez, *Phys. Rev. B* **77**, 125417 (2008).
- <sup>9</sup> R. Roldán, J.-N. Fuchs, and M. O. Goerbig, *Phys. Rev. B* **80**, 085408 (2009).
- <sup>10</sup> R. Roldán, M. O. Goerbig, and J.-N. Fuchs, *Semicond. Sci. Technol.* **25**, 034005 (2010).
- <sup>11</sup> I. B. Bernstein, *Phys. Rev.* **109**, 10 (1958).
- <sup>12</sup> E. Batke, D. Heitmann, J. P. Kotthaus, and K. Ploog, *Phys. Rev. Lett.* **54**, 2367 (1985).
- <sup>13</sup> E. Batke, D. Heitmann, and C. T. Wu, *Phys. Rev. B* **34**, 6951 (1986).
- <sup>14</sup> D. E. Bangert, R. J. Stuart, H. P. Hughes, D. A. Ritchie, and J. E. F. Frost, *Semicond. Sci. Technol.* **11**, 352 (1996).
- <sup>15</sup> S. Holland, C. Heyn, D. Heitmann, E. Batke, R. Hey, K. J. Friedland, and C.-M. Hu, *Phys. Rev. Lett.* **93**, 186804 (2004).
- <sup>16</sup> D. Richards, *Phys. Rev. B* **61**, 7517 (2000).
- <sup>17</sup> K. W. Chiu and J. J. Quinn, *Phys. Rev. B* **9**, 4724 (1974), T. H. Styx, *Theory of plasma waves*, Mc Graw-Hill, 1962.
- <sup>18</sup> K. W. K. Shung, *Phys. Rev. B* **34**, 979 (1986).
- <sup>19</sup> B. Wunsch, T. Stauber, F. Sols, and F. Guinea, *New Journal of Physics* **8**, 318 (2006).
- <sup>20</sup> E. H. Hwang and S. D. Sarma, *Phys. Rev. B* **75**, 205418 (2007).
- <sup>21</sup> F. Stern, *Phys. Rev. Lett.* **18**, 546 (1967).
- <sup>22</sup> M. O. Goerbig, J.-N. Fuchs, K. Kechedzhi, and V. I. Fal’ko, *Phys. Rev. Lett.* **99** (2007).
- <sup>23</sup> A. Wysmolek, D. Plantier, M. Potemski, T. Slupinski, and Z. R. Zytkeiwicz, *Phys. Rev. B* **74**, 165206 (2006).